



# Cold Spring Harbor Protocols

## Interferometric Detection of Action Potentials

Arthur LaPorta and David Kleinfeld

*Cold Spring Harb Protoc*; doi: 10.1101/pdb.ip068148

---

### Email Alerting Service

Receive free email alerts when new articles cite this article - [click here](#).

---

### Subject Categories

Browse articles on similar topics from *Cold Spring Harbor Protocols*.

[Electrophysiology](#) (47 articles)  
[Neural Cell Culture](#) (38 articles)  
[Neuroscience, general](#) (227 articles)

---

---

To subscribe to *Cold Spring Harbor Protocols* go to:  
<http://cshprotocols.cshlp.org/subscriptions>

---

## Information Panel

# Interferometric Detection of Action Potentials

Arthur LaPorta and David Kleinfeld

Individual action potentials in axons can be detected in vitro using intrinsic optical signals. The principles of this detection technique are described here. The technique has been demonstrated using neuronal axons dissected from lobster. It would also be applicable to axons and active dendrites of cultured neurons with diameters somewhat larger than an optical wavelength. Using index-matching techniques, it may be possible to extend the technique to smaller structures.

## INTRODUCTION

Early work showed that light scattering from a network of small neuronal processes is modulated by the propagation of action potentials (Cohen et al. 1968, 1972a,b). Studies of the scattering pattern obtained from a single axon are consistent with a change in the refractive index of the cell membrane. This change is proportional to the voltage across the membrane (Stepnoski et al. 1991) and presumably arises from alignment of dipoles in the membrane. Later work detected displacement of nerves during action potentials (Fang-Yen et al. 2004; Akkin et al. 2007; McCluskey et al. 2007). The magnitude of the change was determined for isolated axons from *Aplysia* neurons, for which the relative change in refractive index was  $\Delta n/n = 50 \times 10^{-6}$  per mV. This corresponds to an equivalent optical phase shift of 0.1 to 0.2 mrad per spike. These relatively small changes could be detected, in single trials, by measuring changes in light scattering with dark-field illumination (Stepnoski et al. 1991).

## PRINCIPLES OF INTERFEROMETRIC DETECTION

The goal of this procedure is to directly confirm the refractive index change by constructing a two-beam interferometer in which a laser beam that passes through an axon interferes with a beam that bypasses the axon. A change in the relative optical phase of the two beams is a measure of the change in total optical density of the preparation. To avoid randomly fluctuating phase shifts, the two beams must be transported by the same optical components. To accomplish this, the apparatus shown in Figure 1A is used. The apparatus uses polarization optics to create two distinct beams that propagate through the same optical system.

A polarization-preserving single-mode optical fiber that transports light from a 5-mW HeNe laser acts as a point source for a microscope objective, producing a collimated Gaussian beam whose linear polarization angle is chosen to be at  $45^\circ$  with respect to the polarization optics that follow. The beam passes through an inclined quartz birefringent plate, which causes a displacement of the S and P

---

Adapted from *Imaging in Neuroscience* (ed. Helmchen and Konnerth). CSHL Press, Cold Spring Harbor, NY, USA, 2011.

© 2012 Cold Spring Harbor Laboratory Press

Cite this article as *Cold Spring Harbor Protoc*; 2012; doi:10.1101/pdb.ip068148

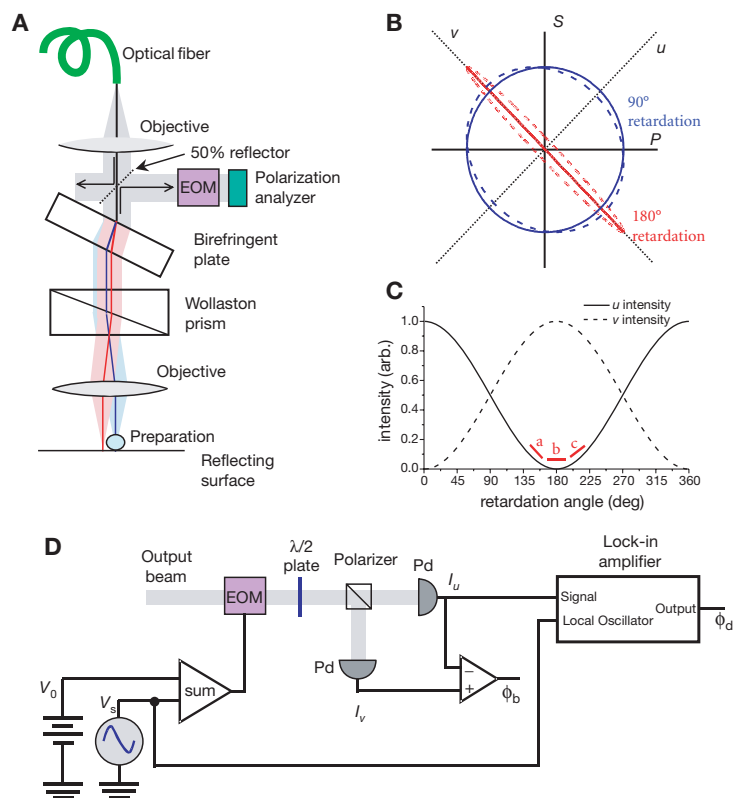


**FIGURE 1.** Schematic of the interferometer and the polarization-based detection system for changes in the optical path length. The interferometric microscope needs to be compact and stiff to avoid uncontrolled fluctuations in the relative phase of the two optical paths, a combination that can be achieved with Microbench components (LINOS Photonics). (A) Essential optics in the interferometer. The broad gray bar represents the total extent of the beam, and the black line represents the central ray. After separation by polarization components, red and blue shading indicates S and P polarization components of the light, respectively. Laser light is introduced via a polarization-preserving optical fiber at the top; this light propagates down to the preparation plane through a microscope objective, polarization components, and a second water-immersion objective. The preparation plane is reflective at the excitation wavelength, and the light is retro-reflected and ultimately coupled out of the microscope using a 50% reflector. The output beam is passed through an electro-optic modulator (EOM) and is detected with a polarization analyzer shown in greater detail in (D). The principles of operation are described in the text. (B) The electric field as a function of optical phase shift, where the S and P axes correspond to the polarization directions of the two rays (red and blue) in (A), and the *u* and *v* axes correspond to the two channels of the polarization analyzer. The projection of the curves on the *u* and *v* axes gives the amplitude of the component that is transmitted to the detectors. (C) The intensity measured by the two channels of the analyzer as a function of optical phase shift. The short red lines are explained in the text. (D) Detailed schematic of the phase-sensitive detection scheme. The EOM introduces a phase shift of the S polarized field with respect to the P polarized field. A DC voltage, denoted as  $V_0$ , is applied to correct for the phase shift of the resting axon. The  $\lambda/2$  plate rotates the polarization state so that the analyzer detects the intensity (*I*) along two diagonal directions, *u* and *v*. For balanced detection, the intensities  $I_u$  and  $I_v$  are nominally equal (see text) and are subtracted to give a phase signal that is denoted as  $\phi_b$ . For dark fringe detection,  $V_0$  is set so that all light goes to the  $I_v$  detector. A phase modulation, denoted as  $V_s$  with frequency  $f_s$ , is superimposed on the EOM drive signal. A deviation of the optical phase from the dark fringe ( $\phi_d$ ) causes a modulation at frequency  $f_s$  to appear in the photocurrent  $I_u$  (see text), which may be detected with a lock-in amplifier (LIA). The modulation signal  $V_s$  is connected to the reference input, and the photocurrent  $I_u$  is connected to the signal input of the LIA, which is configured to measure the in-phase first harmonic component of the signal. The optical phase  $\phi_d$  is obtained from the output of the LIA, which is equal to  $(1/2)I_t(\phi_d)$ , where  $I_t$  is the total intensity.

polarization components with respect to each other. The beams then pass through a Wollaston prism, which introduces a relative angular deviation of the two polarization components, causing them to cross at a point beyond the rear face of the prism. The combined effect of the birefringent plate and the Wollaston prism is similar to that of a Nomarski prism with an unusually large divergence angle. The S and P polarized beams are incident on the rear aperture of a 20× water-immersion

microscope objective. The beam diameters are chosen to match the rear aperture of the objective, and the crossing point is placed at the rear focal plane of the objective. The microscope objective brings the collimated beams to diffraction-limited Gaussian focal spots in the image plane. The angular deviation of the two beams causes the focal spots to occur at distinct positions in the sample plane. The Wollaston angle was chosen to make this separation  $\sim 5 \mu\text{m}$ ; the choice of separation distance depends on the application. Because the two beams cross at the rear focal plane of the objective, their central rays are parallel. The specimen chamber is positioned so that the two beams are normally incident, with their waist at the bottom reflective surface. As a result, the two beams are retro-reflected back into the microscope. The two beams are recombined by the Wollaston and birefringent plate and are coupled out of the apparatus by a 50% reflector.

The beam that emerges from the apparatus consists of a vertical polarization component that has passed through the axon and a horizontal polarization component that has bypassed the axon. The optical phase shift of the resting axon changes the polarization state of the output beam from linear to an arbitrary elliptical state. A change in the optical density or path length of the axon during an action potential would result in a perturbation to the elliptically polarized state.

To detect the small phase shifts expected in response to an action potential, the measurement must employ a differencing scheme to cancel technical fluctuations in the laser light intensity. Here, the output beam is passed through an EOM, which is used to adjust the relative phase shift of the S and P polarization components for the resting neuron. There are two ways the EOM and polarization analyzer may be used (Fig. 1D). The nominal phase shift between the two polarizations may be set to  $90^\circ$ . In this case, the output beam has circular polarization (solid blue curve in Fig. 1B), and the analyzer, which is oriented to measure diagonal components  $I_u$  and  $I_v$ , sees a balanced signal. This corresponds to  $90^\circ$  in Fig. 1C. A deviation in the phase causes a deformation of the circular state (dashed blue curve in Fig. 1B), which imbalances  $I_u$  and  $I_v$ . As a result, the difference signal,  $I_u - I_v$ , is a measure of the phase in which the laser intensity cancels.

A more effective detection method (called the “dark fringe method”) is to set the nominal phase shift between the two polarizations to  $180^\circ$  so that the output state is linearly polarized along  $v$  and the intensity  $I_u$  is 0 (solid red curve in Fig. 1B). An additional phase shift results in a small deviation from linear polarization that causes  $I_u$  to become nonzero. This signal cannot be used directly because the intensity  $I_u \propto 1 + \cos(180^\circ + \phi)$  is second order in the phase  $\phi$  and would have a vanishing signal-to-noise ratio. However, a first-order signal can be obtained by superimposing a sinusoidal modulation of frequency  $f_s$  on the EOM phase shift. For the resting axon, the modulation in the neighborhood of  $180^\circ$  produces no first-order signal in  $I_u$  because the slope of the  $I_u$  versus phase curve is 0 (see line b in Fig. 1C). However, a positive phase shift in the axon would bias the net phase toward higher values (line c in Fig. 1C), where the slope of the curve is positive. In this case, the phase modulation produces a signal at frequency  $f_s$  in  $I_u$  with amplitude proportional to the axon phase shift. Similarly, a negative axon phase would bias the phase toward negative values (line a in Fig. 1C) and produce a modulation with negative amplitude in  $I_u$ . The amplitude of the signal at frequency  $f_s$  (and therefore the axon phase retardation) can be measured using a lock-in amplifier referenced to the EOM modulation signal as shown in Figure 1D. The primary advantage of this technique is that the photodetectors have much less noise near the carrier frequency (chosen to be  $>100 \text{ kHz}$ ) than near DC (0 Hz). In this configuration, both fluctuations in laser intensity and  $1/f$  noise in the photodetectors are avoided, and the principal sources of noise are shot noise and fluctuations in the preparation itself.

## SHORT EXAMPLE OF APPLICATION

Figure 2 shows the preparation chamber for the walking leg nerve dissected from lobster and the optical phase shift recorded from a nerve. The nerve was microdissected so that only a small number of axonal fibers remained in the bundle. The second of the above schemes for phase detection

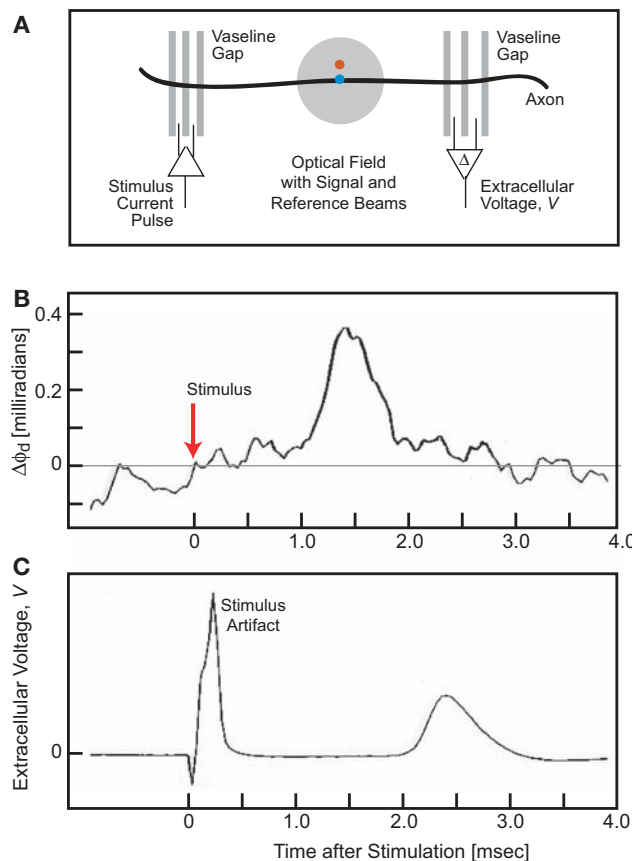


**FIGURE 2.** Results for interferometric measurements through a walking leg nerve from lobster, *Homarus americanus*. The nerve was maintained in artificial seawater. The nerve was microdissected down to a few, but more than one, axonal fibers. (A) The chamber that holds the preparation is a multicompart structure that positions the nerve across a dielectric mirror that has a maximal reflection at 630 nm, close to the HeNe emission line. One beam (P polarization, blue) passes through the nerve, and the second (S polarization, red) passes  $\sim 5\ \mu\text{m}$  away from the nerve. The nerve further rests on two platinum wires at one end, which serve as the voltage stimulation source, and two at the other end, which serve as extracellular recording electrodes. Thin walls with slits that are filled with Vaseline provide electrical isolation between the chambers. (B) The optical signal, denoted by the change in output phase  $\phi_d$  between the two beams, in response to a just-supra-threshold stimulus. Shown is the stimulus-triggered average of 100 samples. (C) The concomitantly measured and averaged electrical signal. The time at which the optical signal is approximately halfway between the application of the stimulus and the detection of the electrical signal at the downstream electrodes. This is consistent with uniform propagation of the action potential along the fibers.

was used. Action potentials were elicited by stimulating the nerve with a voltage pulse set just above threshold; this minimized the number of axons excited. The extracellular signals from the action potential(s) were detected using electrodes placed beyond the imaging point. An optical phase shift of  $\sim 0.4$  mrad was measured after averaging 100 pulses. This signal may contain contributions from more than one axon.

## ADVANTAGES AND LIMITATIONS

The advantage of this technique is that a direct measure of change in optical density is made at a specific point. The measurement is performed in such a way that noise from the measurement process itself (e.g., fluctuations in laser intensity and detector noise) is minimized. The main limitation is that it requires an optically thin, *in vitro* sample; any distortions in the beams degrade the sensitivity of the polarization analyzer. The final signal-to-noise ratio seems to be dominated by fluctuation in the

specimen itself. Although these fluctuations are difficult to quantify, the main causes are probably Brownian motion of the physical structures and biochemical fluctuations in the axon cytoplasm.

## REFERENCES

---

- Akkin T, Joo C, de Boer JF. 2007. Depth-resolved measurement of transient structural changes during action potential propagation. *Biophys J* **94**: 1347–1353.
- Cohen LB, Keynes RD, Hille B. 1968. Light scattering and birefringence changes during nerve activity. *Nature* **218**: 438–441.
- Cohen LB, Keynes RD, Landowne D. 1972a. Changes in axon light scattering that accompany the action potential: Current-dependent components. *J Physiol* **224**: 727–752.
- Cohen LB, Keynes RD, Landowne D. 1972b. Changes in light scattering that accompany the action potential in squid giant axons: Potential-dependent components. *J Physiol* **224**: 701–725.
- Fang-Yen C, Chu MC, Seung HS, Dasari RR, Feld MS. 2004. Non-contact measurement of nerve displacement during action potential with a dual-beam low-coherence interferometer. *Opt Lett* **29**: 2028–2030.
- McCluskey MD, Sable JJ, Foust AJ, Gratton G, Rector DM. 2007. Recording invertebrate nerve activation with modulated light changes. *Appl Optics* **46**: 1866–1871.
- Stepnoski RA, LaPorta A, Raccuia-Behling F, Blonder GE, Slusher RE, Kleinfeld D. 1991. Noninvasive detection of changes in membrane potential in cultured neurons by light scattering. *Proc Natl Acad Sci* **88**: 9382–9386.